Hindawi
Wireless Communications and Mobile Computing
Volume 2020, Article ID 8873912, 16 pages
https://doi.org/10.1155/2020/8873912

Research Article

On the Performance of Wireless Video Communication Using Iterative Joint Source Channel Decoding and Transmitter Diversity Gain Technique

Amaad Khalil,[1] Nasru minallah,[1] Muhammad Asfandyar Awan,[2] Hameed Ullah Khan,[1] Atif Sardar Khan,[1] and Atiq ur Rehman[2]

[1]*Department of Computer Systems Engineering, University of Engineering and Technology Peshawar, Peshawar, Pakistan*
[2]*Division of Information and Computing Technology, College of Science and Engineering, Hamad Bin Khalifa University, Doha, Qatar*

Correspondence should be addressed to Muhammad Asfandyar Awan; mawan@hbku.edu.qa

Received 27 July 2020; Revised 12 November 2020; Accepted 5 December 2020; Published 23 December 2020

Academic Editor: Farman Ullah

In this research work, we have presented an iterative joint source channel decoding- (IJSCD-) based wireless video communication system. The anticipated transmission system is using the sphere packing (SP) modulation assisted differential space-time spreading (DSTS) multiple input-multiple output (MIMO) scheme. SP modulation-aided DSTS transmission mechanism results in achieving high diversity gain by keeping the maximum possible Euclidean distance between the modulated symbols. Furthermore, the proposed DSTS scheme results in a low-complexity MIMO scheme, due to nonemployment of any channel estimation mechanism. Various combinations of source bit coding- (SBC-) aided IJSCD error protection scheme has been used, while considering their identical overall bit rate budget. Artificial redundancy is incorporated in the source-coded stream for the proposed SBC scheme. The motive of adding artificial redundancy is to increase the iterative decoding performance. The performance of diverse SBC schemes is investigated for identical overall code rate. SBC schemes are employed with different combinations of inner recursive systematic convolutional (RSC) codes and outer SBC codes. Furthermore, the convergence behaviour of the employed error protection schemes is investigated using extrinsic information transfer (EXIT) charts. The results of experiments show that our proposed *Rate* – 2/3 SBC-assisted error protection scheme with high redundancy incorporation and convergence capability gives better performance. The proposed *Rate* – 2/3 SBC gives about 1.5 dB E_b/N_0 gain at the PSNR degradation point of 1 dB as compared to *Rate* – 6/7 SBC-assisted error protection scheme, while sustaining the overall bit rate budget. Furthermore, it is also concluded that the proposed *Rate* – 2/3 SBC-assisted scheme results in E_b/N_0 gain of 24 dB at the PSNR degradation point of 1 dB with reference to *Rate* – 1 SBC benchmarker scheme.

1. Introduction

Generally, multimedia communication systems require high data rate, which also results in high demand for transmission power and available bandwidth. Therefore, to transmit wireless multimedia information over limited available bandwidth, high compression efficiency is required. The H.264/AVC codec is a predominant wireless multimedia compression standard because of high compression capabilities required for heterogeneous communication networks and applications [1]. Predictive coding technique and variable-length coding (VLC) increase the H.264/AVC codec compression efficiency required for transmission system, but it also makes the transmitted bitstream more prone to the error [2]. Even a single error in the received bitstream reduces the decoding ability to recover the correct codeword. The predictive coding technique also results in propagating the channel error to its next neighbour video frame. In a wireless system, because of limited bandwidth and varying behaviour of the channel, it makes the video transmission

a difficult task. Layered video coding using unequal equal protection (UEP) technique is used in the H.264 codec for robust video transmission [3]. H.264/AVC with the cross-layered architecture gives better error resilience capability, when used with medium access control (MAC) as discussed in [4]. A transmission system with reversible variable-length codes (RVLC) using irregular convolutional codes (IRCC) that helps in compressing and protecting video codec and uses maximum a posteriori (MAP) algorithm for decoding is discussed in [5]. In [6], the authors discussed convolutional codes with different modulation schemes. Maximum slope (MS) convolutional code is used along with hard and soft decision Viterbi algorithm for decoding. The codeword was mapped to quadrature amplitude modulation (QAM) symbols and quadrature phase shift keying (QPSK) modulation using the additive white Gaussian noise (AWGN) channel. The simulation results of the paper conclude that binary convolutional codes give better results when they were used as inner code in the broadcast channel. Similarly, in [7], the authors have discussed the decrease in energy cost for the communication systems over the wireless channel through an orthogonal coding scheme. Transmission is carried out over the AWGN channel using the differential phase shift keying (DPSK) modulation techniques. The results show a substantial improvement in BER by the use of orthogonal coding and efficient use of transmission signal energy. Furthermore, in [8], the authors have discussed the improvement in concatenated codes. The transmission system employs in its inner code the convolutional code while the outer code comprises of the Hamming code. Block interleaver is used to disperse burst error. The simulation results show better results in BER, when the Hamming code is used as an outer code. The use of space-time coding (STC) to enhance the robustness of data transmission over the wireless channels is investigated in [9]. STC has different coding matrix for multiple input-multiple output (MIMO) transmission, but STBC4 algorithm due to maximum clock transmission steps gives a better peak signal-to-noise ratio (PSNR) and bit error rate (BER). In [10], the authors have presented an H.264/AVC-coded video transmission system using iterative source and channel decoding (ISCD). A novel source bit coding (SBC) and recursive systematic convolutional (RSC) code-assisted IJSCD approach is proposed. The data-partitioned-coded bitstream of H.264/AVC is transmitted with the help of SP-assisted DSTS [10]. The employed SBC scheme improves the performance of our proposed transmission system in the presence of ISCD.

The research paper is organized as fallows. In section 2, we have presented the related works, and section 3 gives details about the H.264/AVC data partitioning. In section 4, we have provided information related to the transmission mechanism of the proposed experimental setup. Section 5 provides the system overview. Furthermore, iterative source and channel decoding are explained in section 6. Details about the EXIT charts are analysed in Section 7, and system performance and results of the paper are presented in Section 8. The conclusion of the paper is presented in section 9.

2. Related Works

Abdullah et al. in [11] debate that H.264/AVC wireless video transmission has problems such as need of higher data networks and error proneness. The study gets its motivation from the use of ultrawide bands for usage of audio-visual signals. The simulations of various scenarios explain the importance of hierarchical and adaptive modulation schemes in various combinations for better video reconstruction. The results from the simulations show a 15 dB increase in PSNR and an increase of 20 dB when added with the various wireless channel adaptive modulation techniques. Nasruminallah et al. in [12] compare three different bandwidth efficient and flexible transceivers for video transmission system using iterative decoding and the simulated Rayleigh channel. The considered three schemes include self-concatenated convolutional, convergent serial concatenated coding, and nonconvergent serial concatenated schemes. Extrinsic information transfer (EXIT) charts show that the SECCC scheme exceeds in performance as compared to the CSCOC and NCSCOC schemes. The BER and PSNR curves also demonstrate that the SECCC scheme performs better for video transmission using iterative decoding. Kadhim et al. in [13] discuss real-time high-quality video transmission with reliability and delay constraints. The typical error protection techniques for example forward error correction and also the automatic repeat request result in the degradation of the video. This paper introduces a partial reliability-based real-time streaming (PERES) technique which is a solution to the application layer that executes partial reliable transfer. The proposed technique consists of acknowledgement and negative acknowledgment system for video transmission and scheduling algorithms with network adaptive algorithms and reliability adaption. Jiyan et al. in [14] propose the design of the H.264 video transmission medium for stationary or mobile user, using the JM tool packet employing the optimization, error protection, and adaptation techniques along the way. The system uses both standard-definition television (SDTV) and high-definition television (HDTV) to input format videos. A complete simulation model with encoder, channel, and decoder is developed. The BER and PSNR values are analysed with varying schemes as GOP, QP, reference frames, and subpixel motion estimation, and the results are shown as graphs. Hadi et al. in [15] present the joint photographic expert group (JPEG2000) image transmission using unequal error protection (UEP) in the presence of polar codes. The proposed transmission scheme achieved better results by using the polarization property of channel codes without significant modification in the overall system. They proposed a joint source channel decoding by using the belief propagation algorithm. The proposed scheme takes the error-resilience tool advantage of the JPEG2000 decoder, which reduces the complexity of system. The experimental results manifest that our designed system has better results as compared to the conventional equal error protection for polar codes. Mhamdi et al. in [16] propose the JPEG2000 image transmission for ISCD using concatenated codes. In this scheme, flexibly UEP is deployed to split the data into several layers so that important source information gets more

protection as compared to less important information. This technique provides better protection along with better decoding performance. The good performance of the designed system is evaluated in the term of a PSNR gain of 10 dB and better subjective quality. The author also presented an adaptive rate allocation scheme which gives better result as compared to static strategy. Hosany suggests in [17] the generalized framework for UEP to evaluate the error performance for rate-compatible puncture convolutional (RCPC) codes and the concatenated Reed-Solomon codes. The transmission system uses 8 PSK modulation schemes in the existence of the Rayleigh fading noise. The designed system uses the MATLAB Simulink and provides better performance with 5 dB difference but increases the overall computational complexity of the system. Chaoui et al. present in [18] the image transmission using joint source channel decoding scheme with arithmetic coding (AC) and resilience technique. The AC technique is very useful in detecting any error occurred in wireless transmission. In the proposed scheme, the JSCD combines the error-detection information feedback of AC decoder with error-free information feedback of the AC decoder. In case of erroneous segment, bit reliabilities are calculated in performing bit back tracking. Bitstream of AC decoder is input to the iterative MPA algorithm, and the result shows 4 to 8 dB better performance as compared to separate source channel model. Balsa proposes [19] the analog JSCD system designed for still images transmission. The proposed system results are compared with digital images such as JPEG and JPEG without entropy. The designed systems show better performance from its alternatives on the basis of the structure similarity (SSIM) index and time required for image transmission. This system does not need to transmit the metadata information, and at the receiver end, analog data is always processed. The proposed analog scheme confirms computational capabilities, low power consumption, and a negligible delay.

3. H.264/AVC

Multimedia transmissions require high compression efficiency owing to limited bandwidth and battery power constraint of wireless systems. Every multimedia application has specific stipulations in terms of compression efficiency, video quality, computational complexity, error resilience, and delay [20]. The H.264/AVC coding scheme is a best solution for such broad-ranged multimedia applications. H.264/AVC is originated as a results of combined efforts of the ITU-T video-coding expert group (VCEG) and International Organization for Standardization (ISO) moving picture experts group (MPEG).The first draft of H.264/AVC was presented in 1999 and after changes in design new draft of this standard was finalized in 2003, which is used for all multimedia application ranging from HD video storage to mobile services. The main goal of introducing this standard is to design a low bit rate and network-friendly video codec that could support a large number of multimedia applications. H.264/AVC delivers better results in terms of robustness in transmission, coding efficiency, and rate distortion efficiency as compared to the predecessor video codecs. H.264/AVC is an efficient video codec design that provides the best performance in real-time communication applications like video conferencing and nonreal-time communication applications like digital television broadcast and video streaming [2].

3.1. H.264/AVC Data Partitioning (DP). Every slice of a macroblock is further subdivided into three partitions based on the importance of data transmission. Data partitioning (DP) is one of the H.264/AVC error resilience techniques in which instead of transmitting the entire video bitstream as a single block video slice, the coded bitstream is partitioned into three slices [2]. The coded information of a macroblock (MB) may be encoded into different video streams called partitions. Each partition has a different sensitivity level. The H.264/AVC video codec supports three different partitions that are types A, B, and C which are discussed below.

(i) *Type A* partitions contain the header information, motion vectors, MB types, and quantization parameters. This partition contains the most sensitive and vulnerable information coded video. If the partition A is corrupted, then B and C are not useful, and the entire partition is counted as a corrupted slice. In such cases, the decoder uses an error concealment technique by using a previously decoded frame of the corresponding video segment [21]

(ii) *Type B* partition carries MB coefficients and MB coded block patterns (CBP) bits of intraframe and represents the chunk of nonzero transform coded coefficients within the block. Bitstream is recovered from errors in the intraframe encoding image regions for certain MBs by switching off interframe prediction. In intraframe coding, the encoding rate is few fractions of MBs, so that is why in this partition, each slice encodes the fewest number of bits [21]

(iii) *Type C* partition holds the interframe motion-compensated error residual (MCER), interframe CBP bits, and uses motion-compensated prediction for encoding MBs bits. In H.264/AVC, the intraframe prediction mode is used for intraframe CBP and intraframe MCER bits for encoding MBs [21].

In the H.264/AVC video codec, partition A is the most vital and essential chunk of video bitstream. In the absence of partition A, it is not possible to decode partitions B and C. Intraframe macroblock information is added in the presence of partition B, with partition A to reconstruct the slice. Similarly, in the presence of partition C with partition A, the reconstructed MCER slice is attached to the motion-compensated slice [21].

4. Transmission Mechanism

The proposed transmission mechanism comprising sphere packing (SP) modulation and differential space-time spreading (DSTS) channel diversity gain technique is presented as follows.

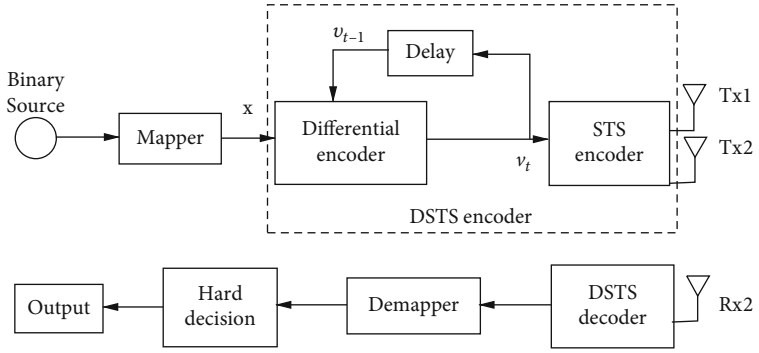

Figure 1: DSTS Encoder.

4.1. Sphere Packing (SP). Sphere packing (SP) modulation is used for modulated symbols to keep the maximum possible Euclidean distance between the modulated symbols. Space-time block code- (STBC-) based orthogonal design of size (2 x 2) for two transmitted antennas are represented as follows.

$$G_2(x_1, x_2) = \begin{bmatrix} x_1 & x_2 \\ x_2' & x_1' \end{bmatrix}, \tag{1}$$

where x_1' represents the complex conjugate of x_1 while column and rows of the above equation represents the spatial dimensions and temporal dimension for two consecutive time slots of two antennas .This scheme consists of two complex modulated symbols (x_1, x_2) that are examined by SP modulation-based orthogonal design for transmission in $T = 2$ time slots from two antennas. The signal is transmitted with L precise space-time signal in consecutive $T = 2$ time slots from the two antennas $(x_{1,l}, x_{2,l}), l = 0, 1, 2 \cdots .L - 1$, where the SP-modulated symbol is represented by L. The aim of jointly designed $x_1 \wedge x_2$ in SP modulation is to enhance the error resilience feature of the system by producing the best minimum Euclidean distance to the remaining $L - 1$ permissible transmitted space-time signals [22].

4.2. Differential Space-Time Spreading (DSTS). The space-time coding (STC) scheme is used to exploit the autonomous fading of the signal of two antennas and create an effectual diversity technique to mitigate the shortcomings of wireless channel. The aim of the STC scheme is to attain a significant power gain and diversity as compared to the single input-single output (SISO) scheme. Space-time block codes (STBC) are a type of STC, proposed by Alamouti [23]. STBC works on a block of data and provides better diversity gain. The STBC technique requires channel estimation and uses coherent detection. Due to the channel estimation technique, the ch4annel experiences an increase in the complexity and cost of the receiver. During transmission, high transmission power is required due to the overhead of fast fading, which increases the number of training symbols. In comparison to this scheme, differential space-time spreading (DSTS) is constituted, which does not require any channel estimation technique. DSTS is a specific scheme for the low-complexity MIMO system by using a noncoherent detection method. The DSTS system gives low complexity, with a trade-off around 3 dB performance loss, as compared to the complex coherent receivers. DSTS consists of two main components that are differential encoder and space-time spreading encoder. In DSTS encoder, the mapped symbols are differentially encoded first and subsequently using STS; they are spread as shown in Figure 1 [23, 24].

At time $t = 0$, the arbitrary dummy reference symbols v_0^1 and v_0^2 are passed to the STS encoder from where these are transmitted via two antennas to the receiver side. Equations (2) and (3) show that the symbols v_t^1 and v_t^2 are differentially encoded as follows [25].

$$v_t^1 = \frac{\left(x_1 \times v_{t-1}^1 + x_2 \times v_{t-1}^{2*}\right.}{\sqrt{\left(\left|v_{t-1}^1\right|^2 + \left|v_{t-1}^2\right|^2\right)}}, \tag{2}$$

$$v_t^2 = \frac{\left(x_1 \times v_{t-1}^2 - x_2 \times v_{t-1}^{1*}\right.}{\sqrt{\left(\left|v_{t-1}^1\right|^2 + \left|v_{t-1}^2\right|^2\right)}}. \tag{3}$$

The differentially encoded symbols are passed to the STS encoder, where symbols are spread assisted by spreading codes c_1 and c_2 and forwarded to antenna for transmission as shown in Figure 2. The spreading code ensures that after using the code concatenation rules, both spreading codes c_1 and c_2 are orthogonal as represented in Equation (4) and (5).

$$c_1^T = [c\, c], \tag{4}$$

$$c_2^T = [c - c]. \tag{5}$$

The differentially encoded symbols split into two substreams, and the two successive symbols are subsequently spread to both antennas for transmission as shown in Figure 2 and represented in Equations (6) and (7).

$$y_t^1 = c_1 \times v_t^1 + c_2 \times v_t^{2*}, \tag{6}$$

$$y_t^2 = c_1 \times v_t^2 - c_2 \times v_t^{1*}. \tag{7}$$

The received signal at a single-receiver antenna is to be denoted by r_t as shown in Equation (8). The nondispersive complex-valued channel impulse response for first and

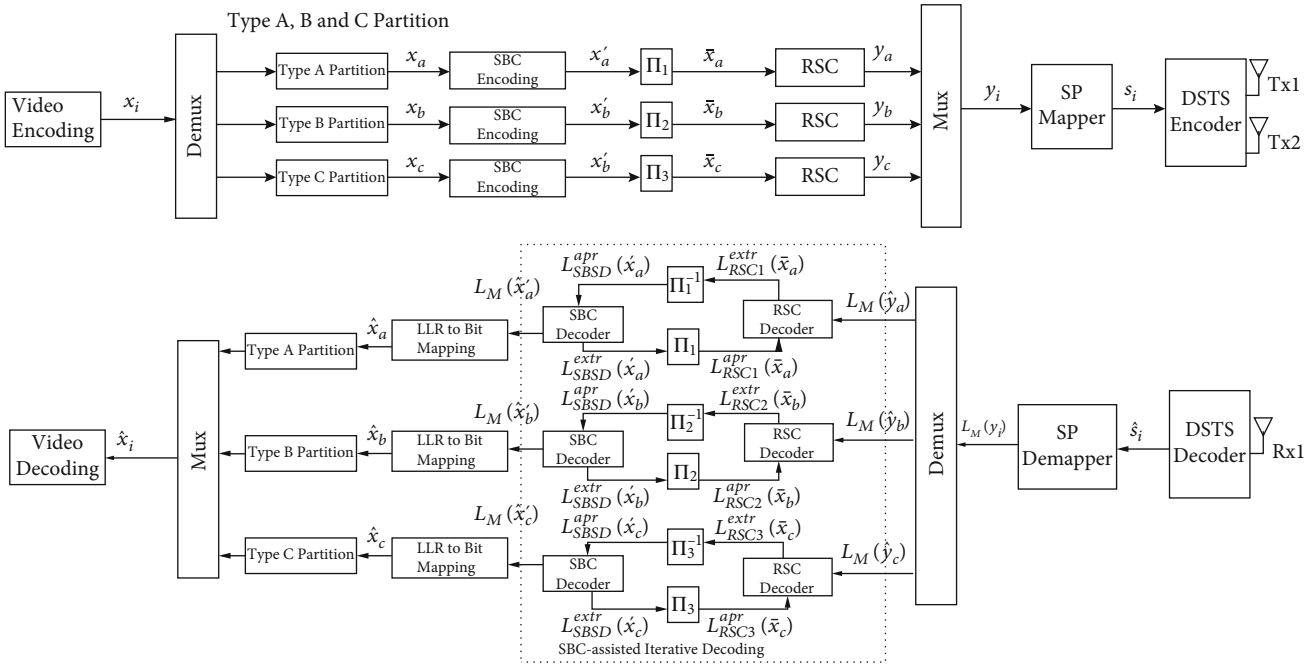

Figure 3: Proposed system design diagram.

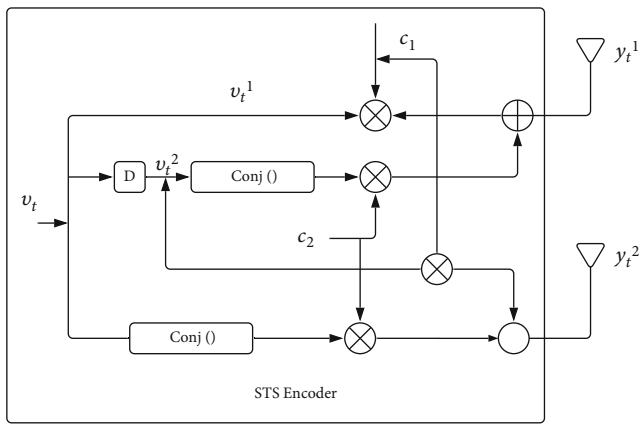

Figure 2: STS encoder.

second antennas is represented by h_1 and h_2. The AWGN channel with a variance of σ_n^2 is denoted by n_t.

$$r_t = h_1 \times y_t^1 + h_2 \times y_t^2 + n_t. \tag{8}$$

In Equations (9) and (10), codes c_1 and c_2 are correlated with received signal r_t, and two data symbols denoted by d_t^1 and d_t^2 are received. H represents the Hermitian matrix.

$$d_t^1 = r_t \times c_1^H = h_1 \times v_t^1 + h_2 \times v_t^2 + c_1^H \times n_t, \tag{9}$$

$$d_t^2 = r_t \times c_2^H = h_1 \times v_t^{2*} - h_2 \times v_t^{1*} + c_2^H \times n_t. \tag{10}$$

Differential decoding is achieved by using received data symbols of successive time slots as shown in Equations (11) and (12). The Gaussian random variables having zero mean complex value are denoted by N_1 and N_2 having a variance of σ_N^2.

$$d_t^1 \times d_{t-1}^{1*} + d_t^{2*} \times d_{t-1}^2 = \left(|h_1|^2 + |h_2|^2\right) \times \sqrt{\left|v_{t-1}^1\right|^2 + \left|v_{t-1}^2\right|^2} \times x_1 + N_1, \tag{11}$$

$$d_t^1 \times d_{t-1}^{2*} - d_t^{2*} \times d_{t-1}^1 = \left(|h_1|^2 + |h_2|^2\right) \times \sqrt{\left|v_{t-1}^1\right|^2 + \left|v_{t-1}^2\right|^2} \times x_2 + N_2. \tag{12}$$

The above equation shows that signal fading (h_1 and h_2) independently works in each transmitter. The proposed technique assures to obtain a diversity gain by the use of a low-complexity algorithm. The space-time spreading operation requires no extra spreading code for transmitting symbols from two antennas in the same time slot.

5. System Overview

In our experimental setup, 300 frames of the H.264-encoded "Akiyo" video sequence are considered for simulation. The diagram of our designed video transmission scheme is presented in Figure 3. The H.264/AVC codec is employed for encoding the video pattern at the transmitter side as shown in Figure 3. The input video sequence has been fragmented by the demultiplexer into three bitstreams, namely Stream A, Stream B, and Stream C. Each stream output contains partition A, B, and C bitstreams in a sequential concatenated manner of all slices of each frame. The output bitstream x_a, x_b, and x_c from demultiplexer are mapped by

Table 1: Different SBC schemes with corresponding symbols and $d_{(\mathrm{H,min})}$.

SBC type	Symbols in decimal	d
Rate – 1 SBC	{0,1}	1
Rate – 2/3 SBC	{0,3,5,6}	2
Rate – 3/4 SBC	{0,3,5,6,10,12,15}	2
Rate – 4/5 SBC	{0,3,5,6,10,12,15,17,18,20,23,24,27,29,30}	2
Rate – 5/6 SBC	{0,3,5,6,10,12,15,17,18,20,23,24,27,29,30,33,34,36,39,40,43,45,46,48,51,53,54,57,58,60,63}	2
Rate – 6/7 SBC	{0, 3, 5, 6, 10, 12, 15, 17, 18, 20, 23, 24, 27, 29, 30, 33, 34, 36, 39, 40, 43, 45, 46, 48, 51, 53, 54, 57, 58, 60 63, 65, 66, 68, 71, 72, 75, 77, 78, 80, 83, 85, 86, 89, 90, 92, 95, 96, 99, 101, 102, 105, 106, 108, 111, 113, 114, 116, 119, 120, 123, 125, 126}	2

using a source bit coding (SBC) scheme into bit strings. Here, $B = b_a + b_b + b_c$, and $a = 1, 2, ..b_a$, $b = 1, 2, ..b_b$, $c = 1, 2, ..b_c$. The bit interleaver Π is used after SBC encoder to interleave the mapped bitstreams and results into $\acute{x}_a$, $\acute{x}_b$, and $\acute{x}_c$. The interleaver within each partition does not affect and extend the video sequence, but it improves the performance of the iterative decoder. Then, the bit strings are encoded with different code rates by the RSC codes, while output streams after channel encoding are represented by y_a, y_b, and y_c. The bitstreams after encoding through RSC error protection codes are multiplexed and concatenated into a single bit steam y_i. The SP mapper is used to transmit the H.624/AVC bitstream with the DSTS encoder using two transmitter antennas. The SP mapper maps the bitstreams to the SP symbol streams represented by s_j as shown in Figure 3. The DSTS provides diversity gain to achieve the coding advantage with low complexity. This process does not need any information of channel estimation, which results in decreasing the BER and improves the subjective video quality. At the receiver end, the DSTS decoder decodes the received signal from the receiving antenna, and the soft information from the DSTS module is forwarded to the SP demapper. Then, the demultiplexer is used to pass the information to the RSC decoder towards its corresponding partition. Each RSC decoder exchanges the extrinsic information with its SBC decoder in the presence of deinterleaver. The deinterleaver helps the SBC decoder module to utilize the residual redundancy. The SBC decoding uses a zero-order Markov model for generating extrinsic information as shown in Equation (13).

$$P\left[\widehat{y}_{(n,k)} \mid y_{(n,k)}\right] = \prod_{i=1}^{n} P\left[\widehat{y}(i)_{(n,k)} \mid y_{(n,k)}\right]. \tag{13}$$

Received n^{th} bit of the k^{th} symbol is represented by $\widehat{y}_{(n,k)}$, and $P[\widehat{y}^{[\mathrm{ext}]}_{(n,k)} \mid y^{[\mathrm{ext}]}_{(n,k)}]$ expresses the extrinsic channel output information as represented in Equation (14).

$$P\left[\widehat{y}^{[\mathrm{ext}]}_{(n,k)} \mid y^{[\mathrm{ext}]}_{(n,k)}\right] = \prod_{i=0, i\neq\lambda}^{n} P\left[\widehat{y}(i)_{(n,k)} \mid y_{(n,k)}\right]. \tag{14}$$

The channel output information and a priori information of the k^{th} symbol give the values of resultant extrinsic *LLR* as represented in Equation (15).

$$LLR\left[y(\lambda)_{(n,k)}\right] = \log\left[\frac{\sum_{y^{[\mathrm{ext}]}_{(n,k)}} P\left(y^{[\mathrm{ext}]}_{(n,k)} \mid y(\lambda)_{(n,k)} = +1\right).P\left[\widehat{y}(i)_{(n,k)} \mid y_{(n,k)}\right]}{\sum_{y^{[\mathrm{ext}]}_{(n,k)}} P\left(y^{[\mathrm{ext}]}_{(n,k)} \mid y(\lambda)_{(n,k)} = -1\right).P\left[\widehat{y}(i)_{(n,k)} \mid y_{(n,k)}\right]}\right]. \tag{15}$$

6. Iterative Joint Source and Channel Decoding

The main goal of iterative joint source and channel decoding (IJSD) is to aid inner and outer decoders in iterative manner to find the maximum possible extrinsic information. SBC uses the residual and artificial redundancy from the encoded bit pattern of video for extraction of extrinsic information. *Rate* – 1 SBC is not capable to achieve better performance gain due to limited redundancy of encoded bitstream. In the H.264/AVC video, to achieve better performance gain in the presence of IJSCD, we add redundant source-coded bits of video, and the method is referred to as the source bit coding (SBC). The SBC scheme is a new approach created on extracting the property of extrinsic information transfer (EXIT) charts. Low BER can be attained by using the iterative decoding method in which there is an EXIT curve in the form of an open tunnel between the inner and outer decoder. To achieve convergence when there exists open tunnel between the inner and outer EXIT curves, they intersect at the upper-right corner of EXIT chart where $(I_A, I_B) = (1, 1)$. Kliewer in [26] discusses the satisfying condition of perfect iterative convergence which is the minimum Hamming distance $d_H = 2$ between the codeword. This encourages the development of an innovative SBC technique where all codewords of SBC have code rate < 1. This can be searched in finding the code table in which necessary condition is $d_H = 2$. This SBC mapping table guarantees that the outer EXIT curve of the SBC outer code will reach with perfect convergence to point $(I_A, I_B) = (1, 1)$. SBC achieves low BER with perfect convergence curve, and its theoretical justification is discussed above. Here, SBC performance analysis is demonstrated with an example in which optimized SBC mapping with *Rate* – 2/3, 3/4, 4/5, 6/7 (as presented in

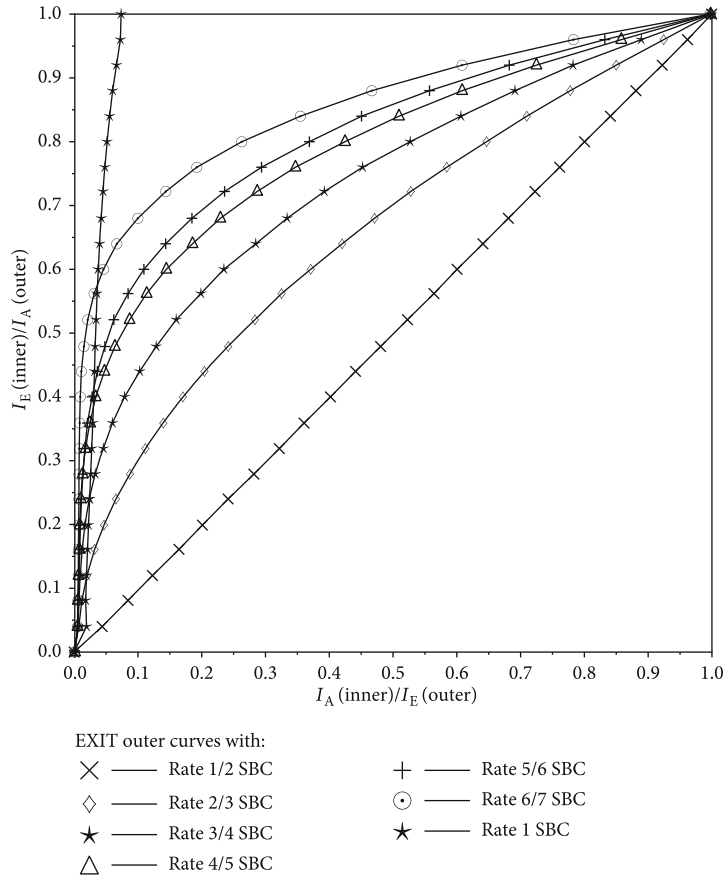

Figure 4: EXIT outer characteristics of different rate SBC coding schemes.

Table 2: Code rate of the different proposed error protection schemes.

S. No.	Outer code (code rate)	Inner code (code rate)	Overall system (code rate)
1	SBC *Rate* – 1	RSC *Rate* – 1/2	*Rate* – 1/2
2	SBC *Rate* – 2/3	RSC *Rate* – 3/4	*Rate* – 1/2
3	SBC *Rate* – 3/4	RSC *Rate* – 2/3	*Rate* – 1/2
4	SBC *Rate* – 4/5	RSC *Rate* – 5/8	*Rate* – 1/2
5	SBC *Rate* – 5/6	RSC *Rate* – 3/5	*Rate* – 1/2
6	SBC *Rate* – 6/7	RSC *Rate* – 7/12	*Rate* – 1/2

Table 1), which is discussed with reference to their EXIT outer curves (as presented in Figure 4). Firstly, it can be observed from the bit mapping presented in Table 1 that all the considered SBC codes of Table 2 ensure the minimum Hamming distance, i.e., $d_H = 2$. As a result, the presented optimized mapping of m to n bit symbols are capable to reach point $(I_A, I_B) = (1, 1)$ of the perfect convergence of the EXIT charts.

7. EXIT Chart Analysis

The inner EXIT characteristic curves of SBC scheme with *R ate* – 1, 2/3, 3/4, 4/5, 6/7 of Table 1 are presented in Figure 4. Figure 4 shows that the EXIT curve for the SBC scheme having code rate < 1 meets at the top-right corner $(I_A, I_B) = (1, 1)$ of the perfect convergence of the EXIT chart. Contrary to this, the *Rate* – 1 SBC scheme falls short of reaching the perfect convergence point. It is important to note that both rate < 1 and *Rate* – 1 SBC scheme maintain an identical bit rate budget for all the employed combinations of outer SBC and inner RSC codes of Table 2. This convergence property of the SBC scheme with rate < 1 is due to the incorporation of artificial residual redundancy in the SBC coding process. Therefore, logically it is clear that rate < 1 SBC is potentially capable to take the maximum advantage of the iterative decoding mechanism by exchanging the beneficial mutual information to achieve lower BER. On the other hand, EXIT curves for SBC scheme with *Rate* – 1 fail to reach and meet at the top-right corner and are not capable to gain any advantage of

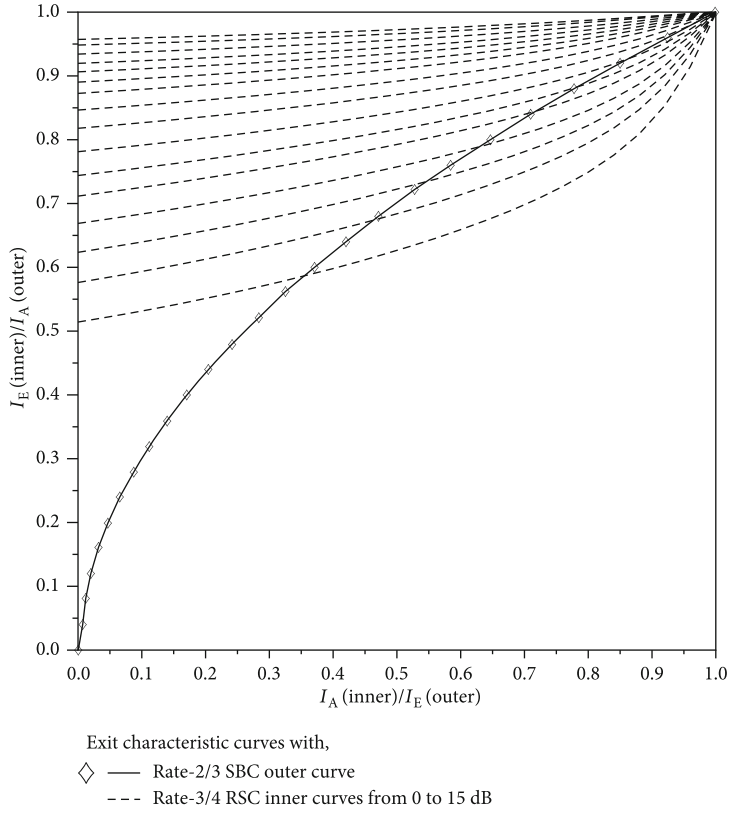

Figure 5: EXIT characteristics curves with *Rate* – 2/3 SBC outer code and *Rate* – 3/4 RSC inner code.

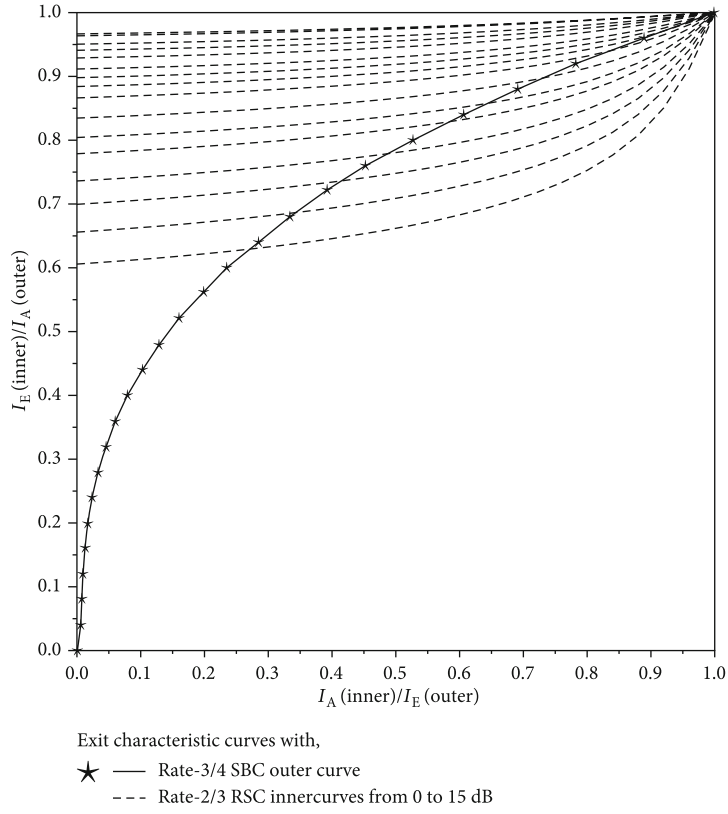

Figure 6: EXIT characteristics curves with *Rate* – 3/4 SBC outer code and *Rate* – 2/3 RSC inner code.

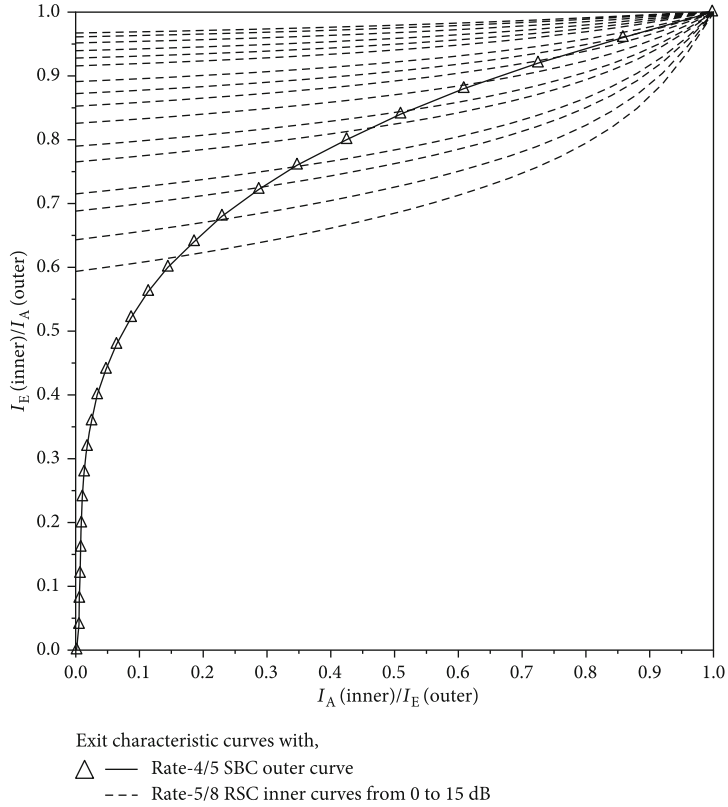

Figure 7: EXIT characteristics curves with *Rate* – 4/5 SBC outer code and *Rate* – 5/8 RSC inner code.

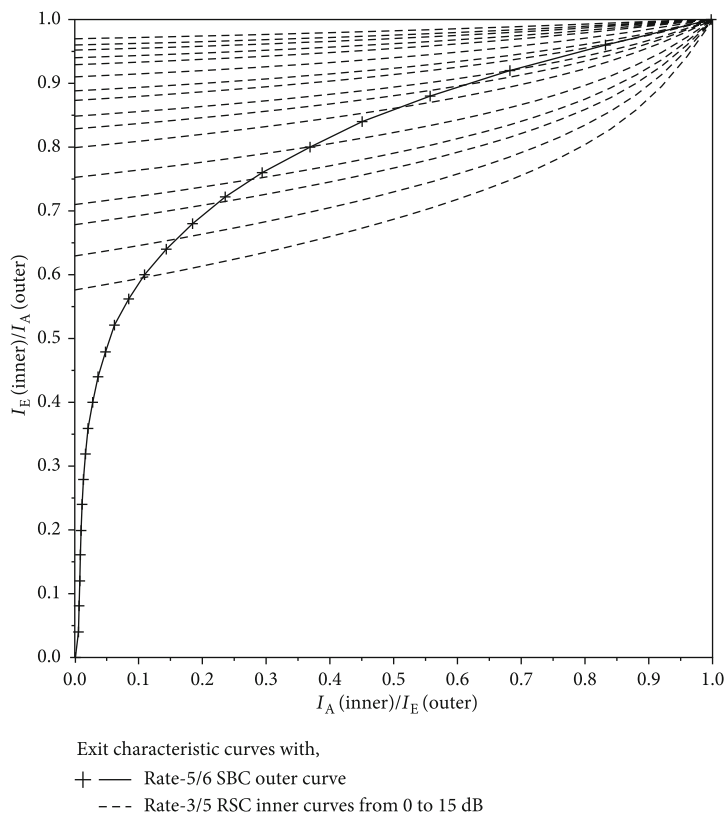

Figure 8: EXIT characteristics curves with *Rate* – 5/6 SBC outer code and *Rate* – 3/5 RSC inner code.

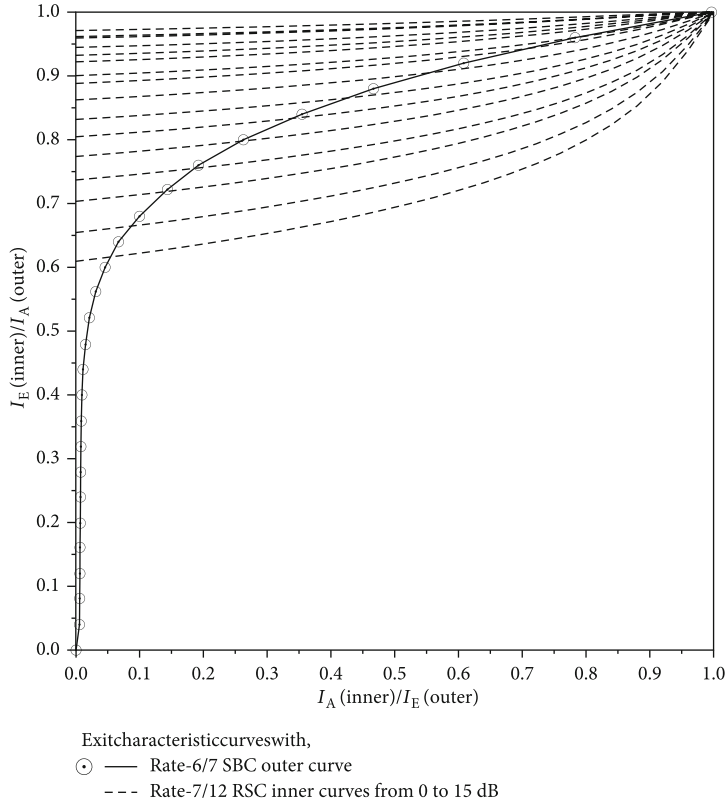

Figure 9: EXIT characteristics curves with *Rate* – 6/7 SBC outer code and *Rate* – 7/12 RSC inner code.

the iterative decoding procedure. With reference to the EXIT outer curves of Figure 4, generated for the different SBC schemes of Table 1, their EXIT characteristic curves along with the corresponding inner RSC curves are presented in Figures 5–9. The presented EXIT characteristic curve shows that the open EXIT tunnel approaches closer to point $(I_A, I_B) = (1, 1)$ of the perfect convergence while employing lower rate SBC as compared to the relatively high rate SBC scheme for the same E_b/N_0 value. More specifically, considering an E_b/N_0 value of 4 dB, the open EXIT tunnel for *Rate* – 2/3 SBC with *Rate* – 3/4 RSC reaches to point $(I_A, I_B) = (0.72,0.85)$ as presented in Figure 5. Similarly, the EXIT tunnels for *Rate* – 3/4, 4/5, 5/6, 6/7 SBC with corresponding RSC code *Rate* – 2/3, 5/8, 3/5, 7/12 of Table 2 reach to points $(I_A, I_B) = (0.6,0.85), (0.47,0.8)$, and $(0.38,0.8)$, respectively. Hence, it can be concluded that the open EXIT tunnel feature of the SBC as the outer decoder and RSC as the inner decoder is more promising while considering a lower rate SBC of Table 2.

Table 3: Systems parameters.

Systems parameters	Value
Source coding	H.264/AVC
Frame rate (fps)	15
Bit rate (kbps)	64
No. of MB's/slice	11
No. of slices/frame	9
Intraframe MB update/frame	3
Channel coding	RSC
Overall code rate	½
MIMO scheme	DSTS
Modulation scheme	SP ($L = 16$)
Number of transmitters	2
Number of receivers	1
Spreading code	Walsh code
Spreading factor	8
Number of users	4
Channel	Correlated Rayleigh fading
Normalized Doppler frequency	0.01

8. System Performance and Results

This part of the paper deals with the explanation of the performance outcome for the suggested schema. The "Akiyo" video pattern [1] contains a quarter common intermediate format (QCIF) of 45 frames, and each frame is 176x144 pixels. The video uses the H.264/AVC JM 19 video codec for encryption, and it is encoded with 64 kbps bit rate for our test sequence at 15 frames per second. Every single QCIF frame is divided into nine segments, and every segment consists of a row of 11 MBs within each QCIF frame. The resultant video sequence contains an intracoded "I" frame, and then 44 predicted frames "P" are placed such that the IPPP

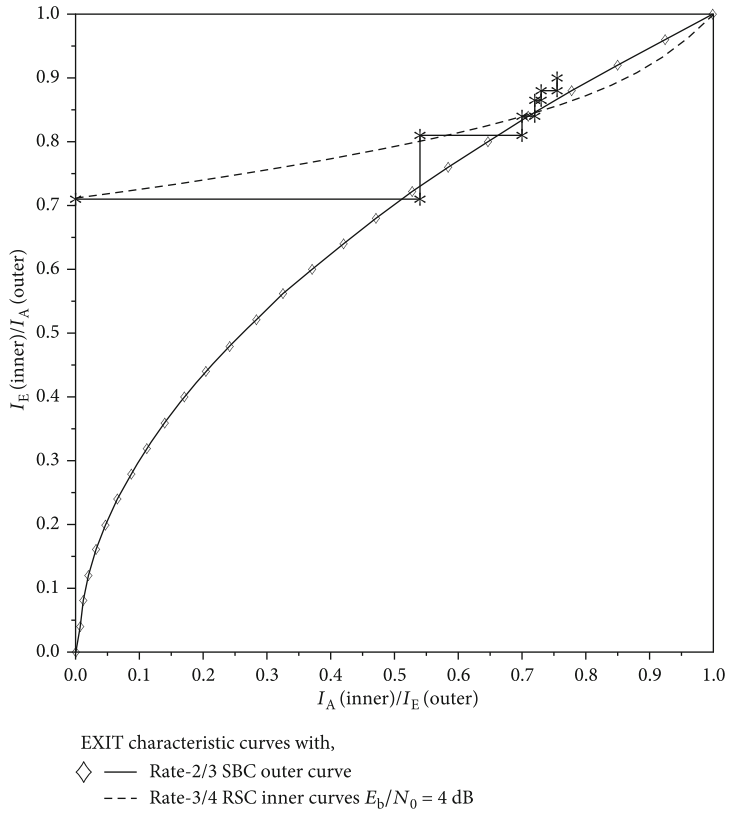

Figure 10: EXIT chart and simulated decoding trajectory of *Rate* – 2/3 SBC scheme of Table 2.

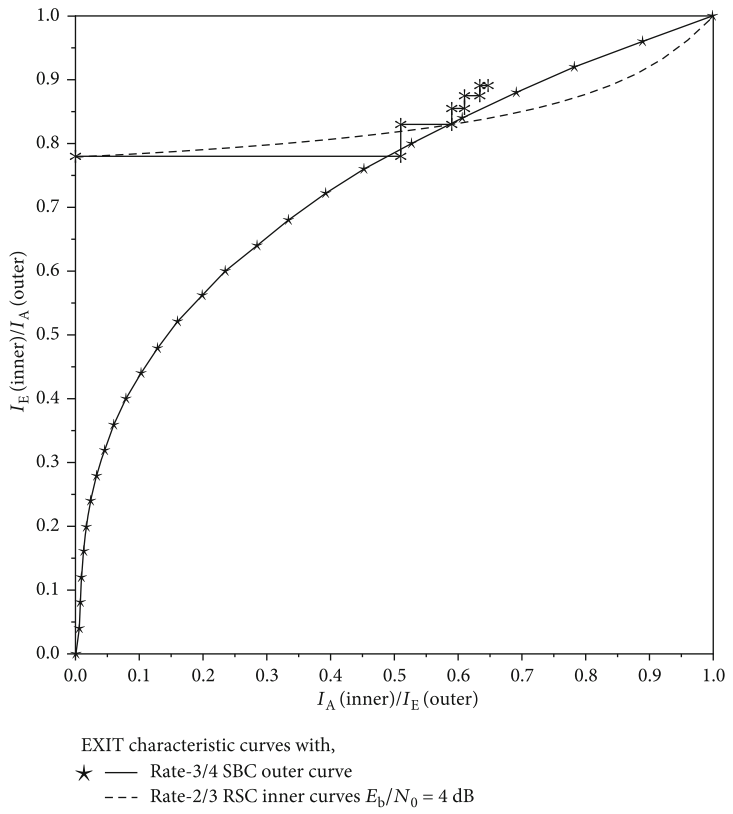

Figure 11: EXIT chart and simulated decoding trajectory of *Rate* – 3/4 SBC scheme of Table 2.

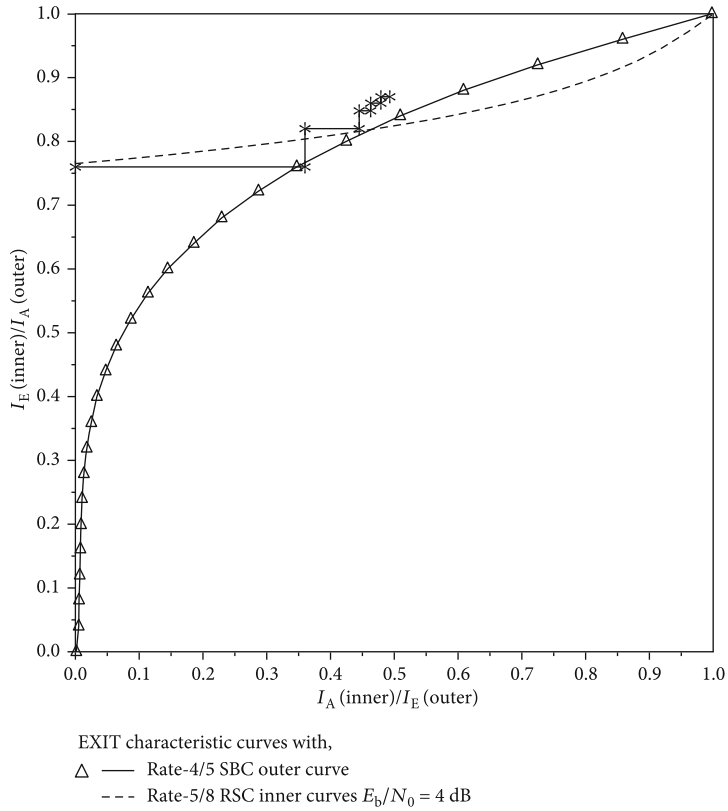

Figure 12: EXIT chart and simulated decoding trajectory of *Rate* – 4/5 SBC scheme of Table 2.

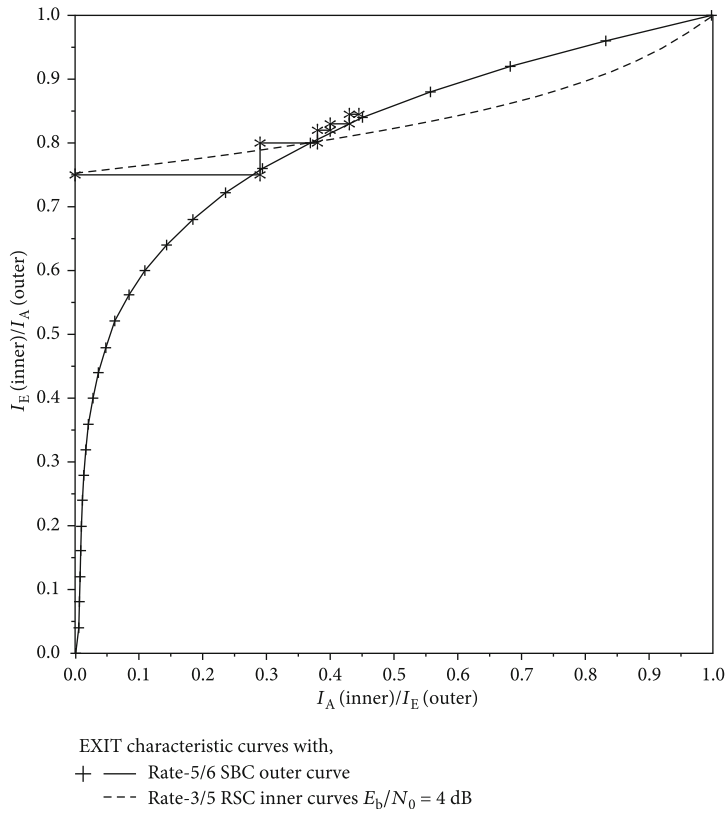

Figure 13: EXIT chart and simulated decoding trajectory of *Rate* – 5/6 SBC scheme of Table 2.

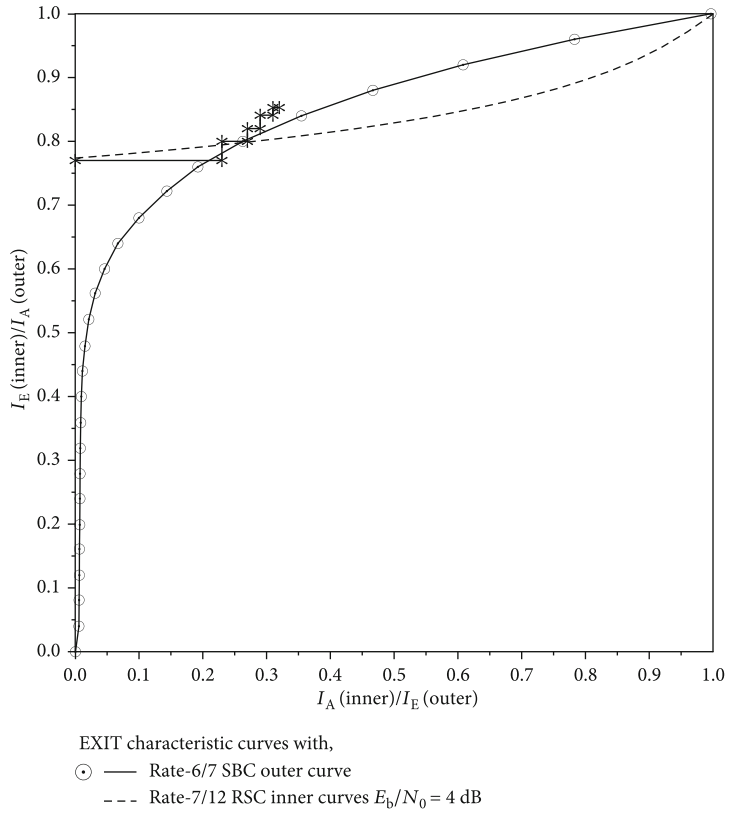

Figure 14: EXIT chart and simulated decoding trajectory of *Rate* – 6/7 SBC scheme of Table 2.

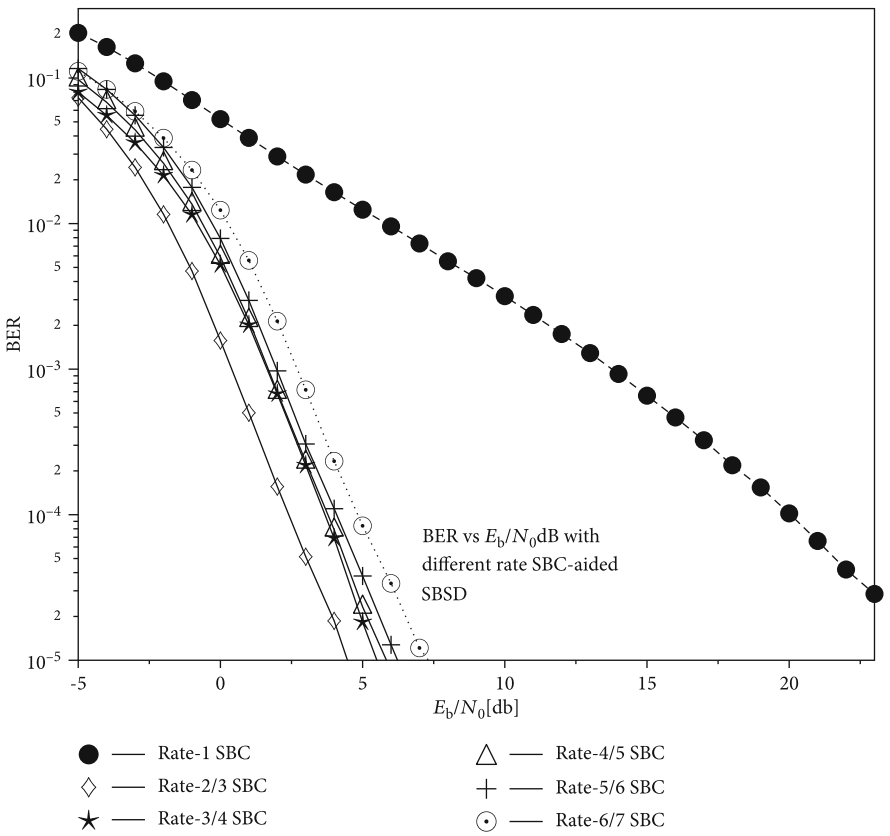

Figure 15: BER performance curves of the coding scheme presented in Table 2.

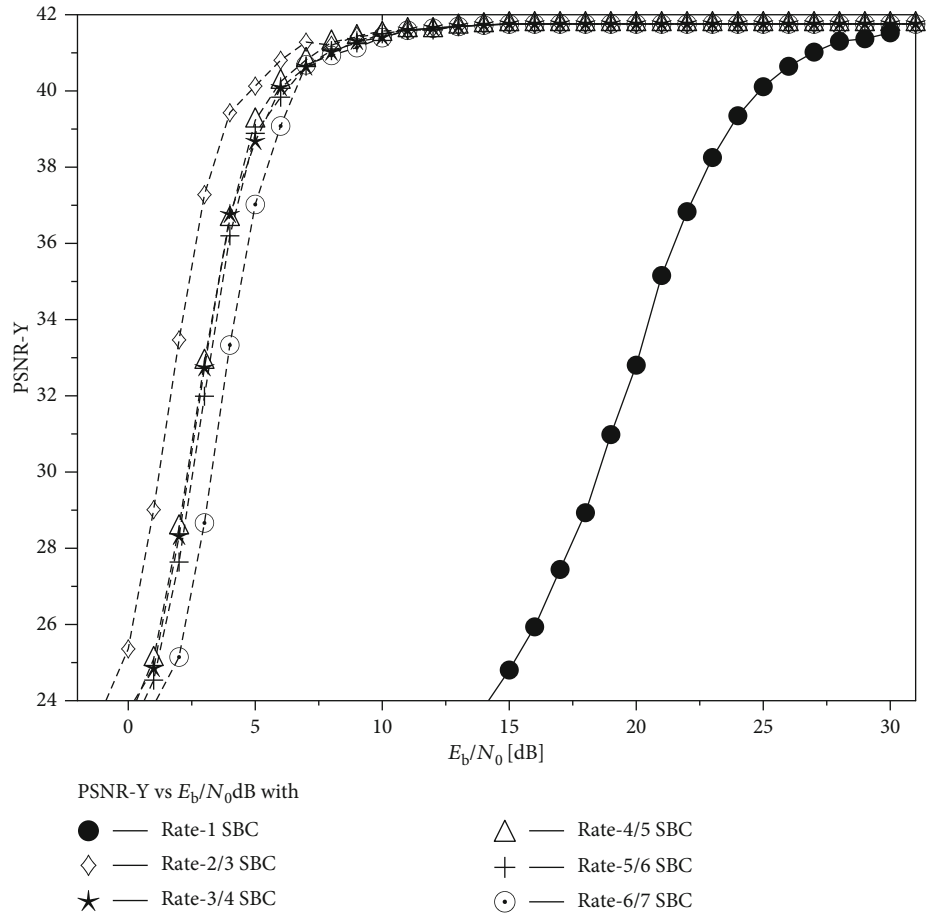

Figure 16: PSNR performance curves of the coding scheme presented in Table 2.

PP… frame sequence is considered in which the "I" frame is repeated after 45 frames within a 3-second duration at 15 frames per second. The intracoded frame has additional benefits in controlling error propagation, so that is why our considered video sequence has a special pattern of "I" and "P" frames. Details about the system parameters of this proposed experimental scheme are presented in Table 3. Flexible macroblock ordering (FMO) and various reference frames utilization, employed for the interframe motion compensation, with additional computational complexity do not have processing performance in a low bit rate video telephony video sequence. Therefore, they were not considered for our H.264/AVC-coded video stream. Source bitstream contains limited residual redundancy. The Monte Carlo simulations were carried out using 45 frames of the "Akiyo" video sequence; experiments were repeated for 260 times, and the average results are considered. SBC with $Rate - 1$ mapping has limited residual redundancy in the coded stream, and therefore, the number of iterations is limited to $I = 3$. For SBC with rate < 1, as presented in Table 1, the mapping obeys the necessary and sufficient condition to reach the upper-right corner of the EXIT chart, and hence, the number of iterations is fixed to $I = 5$. The performance of the various error protection schemes with diverse SBC coding rate was evaluated with the overall same video rate and code rate. From the perspective of H.264/AVC coding, it is pertinent to know that when the frames of low-motion video clips are corrupted due to loss of partition A, the corresponding partitions B and C are not usable, and hence, they are also dropped and the previously decoded frame is used for concealment. A mechanism of motion-compensated prediction is utilized to conceal the lost segment of the future frames. However, a scenario where partition A is received correctly, with loss of partition B of the corresponding video segment, will result in loss of intraframe-coded MB information contained in partition B and hence will result in loss of quality of the corresponding video sequence. The decoding trajectories for the $Rate - 2/3, 3/4, 4/5, 6/7$ SBC schemes of Table 2 are recorded at $E_b/N_0 = 4$ dB as shown in Figures 10–14. Performance analysis of the designed systems using the SBC mapping $Rate - 2/3, 3/4, 4/5, 6/7$ and $Rate - 1$ on the basis of achievable BER and PSNR is shown in Figures 15 and 16, respectively. The SBC $Rate - 2/3$ scheme, with highest redundancy incorporation capability, results in the best BER performance as compared to the other coding schemes of Table 2. Furthermore, it is also observed that the $Rate - 1$ SBC scheme along with $Rate - 1/2$ RSC as inner coding scheme results in worst BER performance, due to its nonconvergence capability in the iterative decoding process. Moreover, it is4 also observed that owing to best BER performance of the

Rate – 2/3 SBC coding scheme, it results in its best PSNR performance, relative to the counterpart coding schemes of Table 2, as shown in Figure 16. More specifically, the *Rate* – 2/3 SBC scheme results in E_b/N_0 gain of 1.5 dB at the PSNR degradation point of 1 dB as compared to the *Rate* – 6/7 SBC scheme having an equivalent overall bit rate. Furthermore, it is also observed from Figure 15 that the proposed *Rate* – 2/3 SBC scheme results in E_b/N_0 gain of 24 dB, with reference to the benchmarker *Rate* – 1 SBC coding scheme, at the PSNR degradation point of 1 dB. Furthermore, it is important to note that both the *Rate* – 2/3 and *Rate* – 1 SBC coding schemes are having an identical overall code rate.

9. Conclusion

In this research work, data-partitioned H.264/AVC video bitstream is transmitted using the iterative joint source and channel decoding (IJSCD) scheme. The performance of different diverse-rated SBC outer-coding schemes was investigated in combination with RSC inner codes, while keeping the overall bit rate budget constant. The source- and channel-coded video stream is SP modulated and transmitted using the DSTS-assisted transceiver. It was demonstrated that the designed IJSCD scheme using the *Rate* – 2/3 SBC scheme gives better BER performance due to incorporation of high level of redundancy in the source bitstream. The convergence behaviour of the presented IJSCD error protection schemes is investigated with the aid of the EXIT charts. The experimental result shows that our *Rate* – 2/3 SBC-assisted error protection scheme with high redundancy incorporation capability gives better results with about 1.5 dB E_b/N_0 gain at the PSNR degradation point of 1 dB as compared to *Rate* – 6/7 SBC-assisted error protection scheme while maintaining the overall bit rate budget constant. Furthermore, it is also concluded that the proposed *Rate* – 2/3 SBC-assisted scheme results in E_b/N_0 gain of 24 dB at E_b/N_0 degradation point of 1 dB with reference to the *Rate* – 1 SBC benchmarker scheme.

Data Availability

The authors approve that data used to support the finding of this study are included in the article.

Conflicts of Interest

The authors declare that they have no known competing financial interests or personal relationships that could have appeared to influence the work reported in this paper.

Acknowledgments

This research work is funded by the National Center of Big Data and Cloud Computer (NCBC), University of Engineering and Technology, Peshawar, under the auspices of Higher Education Commission, Pakistan.

References

[1] L. Hanzo, P. Cherriman, and J. Streit, *Video Compression and Communications: From Basics to H.261, H.263, H.264, MPEG2, MPEG4 for DVB and HSDPA-Style Adaptive Turbo Transceivers*, Wiley-IEEE Press, 2007.

[2] T. Stockhammer, M. M. Hannuksela, and T. Wiegand, "H.264/AVC in wireless environments," *IEEE Transactions on Circuits and Systems for Video Technology*, vol. 13, no. 7, pp. 657–673, 2003.

[3] M. M. Ghandi, B. Barmada, E. V. Jones, and M. Ghanbari, "H.264 layered coded video over wireless networks: channel coding and modulation constraints," *EURASIP Journal on Advances in Signal Processing*, vol. 2006, no. 1, Article ID 085870, 2006.

[4] A. Ksentini, M. Naimi, and A. Gueroui, "Toward an improvement of H.264 video transmission over IEEE 802.11e through a cross-layer architecture," *IEEE Communications Magazine*, vol. 44, no. 1, pp. 107–114, 2006.

[5] A. Q. Pham, J. Wang, L. L. Yang, and L. Hanzo, "An iterative detection aided irregular convolutional coded wavelet videophone scheme using reversible variable-length codes and map equalization," in *2007 IEEE 65th Vehicular Technology Conference - VTC2007-Spring*, pp. 2404–2408, Dublin, Ireland, April 2007.

[6] V. V. Zyablov and V. G. Potapov, "Error correcting coding schemes for a broadcast channels," in *XVI International Symposium "Problems of Redundancy in Information and Control Systems" (REDUNDANCY)*, pp. 32–35, Moscow, Russia, Russia, October 2019.

[7] A. V. Rabin, "Encoding and decoding schemes in communication systems using orthogonal coding for noise immunity's increase," in *Wave Electronics and its Application in Information and Telecommunication Systems (WECONF)*, pp. 1–4, IEEE, Saint-Petersburg, Russia, 2019.

[8] S. Jihwan and H. Lee, "Burst error correction for convolutional code concatenated with Hamming code with a block interleaver," in *International Conference on Artificial Intelligence in Information and Communication (ICAIIC)*, pp. 531–533, Fukuoka, Japan, February 2020.

[9] M. Ivanov, A. Timoshenko, N. B. Molenkamp, and M. Sokolov, "Implementation of space-time coding model for communication systems MIMO 4x4," in *2020 IEEE Conference of Russian Young Researchers in Electrical and Electronic Engineering (EIConRus)*, pp. 1700–1702, St. Petersburg and Moscow, Russia, January 2020.

[10] M. EL-Hajjar, O. Alamri, S. X. Ng, and L. Hanzo, "Turbo detection of precoded sphere packing modulation using four transmit antennas for differential space-time spreading," *IEEE Transactions on Wireless Communications*, vol. 7, no. 3, pp. 943–952, 2008.

[11] A. B. Abdullah, A. Zibri, A. Dziri, and F. Tlili, "H.264/AVC video transmission over UWB AV PHY IEEE 802.15.3c using UEP and adaptive modulation techniques," in *International Conference on Advanced Communication Technologies and Networking (CommNet)*, Rabat, Morocco, April 2019.

[12] N. Minallah, M. F. U. Butt, I. U. Khan et al., "Analysis of near-capacity iterative decoding schemes for wireless communication using EXIT charts," *IEEE Access*, vol. 8, pp. 124424–124436, 2020.

[13] H. F. Kadhim, A. H. A. Mahmood, and N. K. Nasser, "H.264 video transmission with high quality and low bitrate over wireless network," *International Advanced Research Journal in Science, Engineering and Technology*, vol. 5, no. 5, 2018.

[14] W. Jiyan, T. Rui, and W. Ming, "Streaming high-definition real-time video to mobile devices with partially reliable

transfer," *IEEE Transactions on Mobile Computing*, vol. 18, no. 2, pp. 458–472, 2019.

[15] A. Hadi, E. Alsusa, and A. Al-Dweik, "Information unequal error protection using polar codes," *IET Communications*, vol. 12, no. 8, pp. 956–961, 2018.

[16] M. Mhamdi, A. Zribi, C. Perrine, and Y. Pousset, "Efficient multiple concatenated codes with turbo-like decoding for UEP wireless transmission of scalable JPEG 2000 images," *IEEE Access*, vol. 7, pp. 6327–6336, 2019.

[17] M. A. Hosany, "Performance evaluation of an unequal concatenated error protection system for the HEVC standard over wireless channels," *Arabian Journal for Science and Engineering*, vol. 45, no. 8, pp. 6489–6500, 2020.

[18] S. Chaoui, O. Ouda, and C. Hamrouni, "A joint source channel decoding for image transmission," *Advances in Science, Technology and Engineering Systems Journal*, vol. 4, no. 6, pp. 183–191, 2019.

[19] J. Balsa, T. Domínguez-Bolaño, O. Fresnedo, J. A. García-Naya, and L. Castedo, "Transmission of still images using low-complexity analog joint source-channel coding," *Sensors*, vol. 19, no. 13, p. 2932, 2019.

[20] S. Wenger, "H.264/AVC Over IP," *IEEE transactions on circuits and systems for video technology*, vol. 13, no. 7, pp. 645–656, 2003.

[21] T. Stockhammer and M. Bystrom, "H.264/AVC data partitioning for mobile video communication," in *2004 International Conference on Image Processing, 2004. ICIP '04.*, pp. 545–548, Singapore, October 2004.

[22] J. H. Conway and N. J. A. Sloane, *Sphere Packings, Lattices, and Groups*, Springer-Verlag, New York, USA, 1999.

[23] S. M. Alamouti, "A simple transmit diversity technique for wireless communications," *IEEE Journal on Selected Areas in Communications*, vol. 16, no. 8, pp. 1451–1458, 1998.

[24] B. Hochwald, T. L. Marzetta, and C. B. Papadias, "A transmitter diversity scheme for wideband CDMA systems based on space-time spreading," *IEEE Journal on Selected Areas in Communications*, vol. 19, no. 1, pp. 48–60, 2001.

[25] M. El-Hajjar, O. Alamri, and L. Hanzo, "Differential space-time spreading using iteratively detected sphere packing modulation and two transmit antennas," in *IEEE Wireless Communications and Networking Conference, 2006. WCNC 2006.*, pp. 1664–1668, Las Vegas, NV, USA, April 2006.

[26] R. G. Maunder, J. Kliewer, S. X. Ng, J. Wang, L. Yang, and L. Hanzo, "Joint iterative decoding of trellis-based VQ and TCM," *IEEE Transactions on Wireless Communications*, vol. 6, no. 4, pp. 1327–1336, 2007.